University of Nebraska - Lincoln
DigitalCommons@University of Nebraska - Lincoln

US Department of Energy Publications | US Department of Energy

1-1-2011

Purification and Characterization of the [NiFe]-Hydrogenase of *Shewanella oneidensis* MR-1

Liang Shi
Pacific Northwest National Laboratory, liang.shi@pnnl.gov

Sara M. Belchik
Pacific Northwest National Laboratory

Andrew E. Plymale
Pacific Northwest National Laboratory

Steve Heald
Argonne National Laboratory

Alice C. Dohnalkova
Pacific Northwest National Laboratory

See next page for additional authors

Follow this and additional works at: http://digitalcommons.unl.edu/usdoepub

Part of the Bioresource and Agricultural Engineering Commons

Shi, Liang; Belchik, Sara M.; Plymale, Andrew E.; Heald, Steve; Dohnalkova, Alice C.; Sybirna, Kateryna; Bottin, Herve; Squier, Thomas C.; Zachara, John M.; and Fredrickson, James K., "Purification and Characterization of the [NiFe]-Hydrogenase of *Shewanella oneidensis* MR-1" (2011). *US Department of Energy Publications.* Paper 182.
http://digitalcommons.unl.edu/usdoepub/182

This Article is brought to you for free and open access by the US Department of Energy at DigitalCommons@University of Nebraska - Lincoln. It has been accepted for inclusion in US Department of Energy Publications by an authorized administrator of DigitalCommons@University of Nebraska - Lincoln.

Authors
Liang Shi, Sara M. Belchik, Andrew E. Plymale, Steve Heald, Alice C. Dohnalkova, Kateryna Sybirna, Herve Bottin, Thomas C. Squier, John M. Zachara, and James K. Fredrickson

This article is available at DigitalCommons@University of Nebraska - Lincoln: http://digitalcommons.unl.edu/usdoepub/182

This article is a U.S. government work, and is not subject to copyright in the United States.

APPLIED AND ENVIRONMENTAL MICROBIOLOGY, Aug. 2011, p. 5584–5590 Vol. 77, No. 16
0099-2240/11/$12.00 doi:10.1128/AEM.00260-11
Copyright © 2011, American Society for Microbiology. All Rights Reserved.

Purification and Characterization of the [NiFe]-Hydrogenase of *Shewanella oneidensis* MR-1[▽]

Liang Shi,[1]* Sara M. Belchik,[1] Andrew E. Plymale,[1] Steve Heald,[2] Alice C. Dohnalkova,[1] Kateryna Sybirna,[3] Hervé Bottin,[3] Thomas C. Squier,[1] John M. Zachara,[1] and James K. Fredrickson[1]

Pacific Northwest National Laboratory, Richland, Washington 99352[1]; Argonne National Laboratory, Argonne, Illinois 60439[2]; and CEA, DSV, iBiTec-S, SB2SM, LPB (URA CNRS 2096), 91191 Gif-sur-Yvette Cedex, France[3]

Received 4 February 2011/Accepted 21 June 2011

***Shewanella oneidensis* MR-1 possesses a periplasmic [NiFe]-hydrogenase (MR-1 [NiFe]-H_2ase) that has been implicated in H_2 production and oxidation as well as technetium [Tc(VII)] reduction. To characterize the roles of MR-1 [NiFe]-H_2ase in these proposed reactions, the genes encoding both subunits of MR-1 [NiFe]-H_2ase were cloned and then expressed in an MR-1 mutant without *hyaB* and *hydA* genes. Expression of recombinant MR-1 [NiFe]-H_2ase in *trans* restored the mutant's ability to produce H_2 at 37% of that for the wild type. Following purification, MR-1 [NiFe]-H_2ase coupled H_2 oxidation to reduction of $Tc(VII)O_4^-$ and methyl viologen. Change of the buffers used affected MR-1 [NiFe]-H_2ase-mediated reduction of $Tc(VII)O_4^-$ but not methyl viologen. Under the conditions tested, all $Tc(VII)O_4^-$ used was reduced in Tris buffer, while in HEPES buffer, only 20% of $Tc(VII)O_4^-$ was reduced. The reduced products were soluble in Tris buffer but insoluble in HEPES buffer. Transmission electron microscopy analysis revealed that Tc precipitates reduced in HEPES buffer were aggregates of crystallites with diameters of ~5 nm. Measurements with X-ray absorption near-edge spectroscopy revealed that the reduction products were a mixture of Tc(IV) and Tc(V) in Tris buffer but only Tc(IV) in HEPES buffer. Measurements with extended X-ray adsorption fine structure showed that while the Tc bonding environment in Tris buffer could not be determined, the Tc(IV) product in HEPES buffer was very similar to $Tc(IV)O_2 \cdot nH_2O$, which was also the product of $Tc(VII)O_4^-$ reduction by MR-1 cells. These results shows for the first time that MR-1 [NiFe]-H_2ase catalyzes $Tc(VII)O_4^-$ reduction directly by coupling to H_2 oxidation.**

Under anoxic conditions, the gammaproteobacterium *Shewanella oneidensis* MR-1 (MR-1) can couple oxidation of organic matter and H_2 to reduction of oxidized metals, such as ferric iron [Fe(III)] and manganese [Mn(IV)], and metal contaminants, including technetium [Tc(VII)], uranium [U(VI)], and chromium [Cr(VI)] (15, 20, 21, 23, 24, 27–30, 41). Phenotypic analyses of MR-1 mutants reveal that while multiheme *c*-type cytochromes, such as MtrC and OmcA, are directly involved in reduction of Fe(III) oxides, Tc(VII), U(VI), and Cr(VI), [NiFe]-hydrogenase ([NiFe]-H_2ase) has also been implicated in Tc(VII) reduction (2, 3, 6, 23, 24, 31). Biochemical characterization of purified proteins demonstrated that MtrC and/or OmcA could bind to the surface of crystalline Fe(III) oxide hematite (α-Fe_2O_3) and reduce hematite as well as Tc(VII), U(VI), Cr(VI), and chelated Fe(III), providing direct evidence that MtrC and OmcA can serve as terminal reductases for extracellular reduction of these oxidized metals and metal contaminants (2, 10, 13, 17, 19, 25, 35, 36, 40, 42). MR-1 [NiFe]-H_2ase is believed to be localized in the periplasm, where it has been implicated in both H_2 formation and oxidation in addition to Tc(VII) reduction (24, 26). However, in contrast to well-studied MtrC and OmcA, whether MR-1 [NiFe]-H_2ase can catalyze H_2 formation and oxidation and Tc redox transformation remains unclear because it has not been purified or characterized.

Unlike MtrC and OmcA, which can be expressed under aerobic conditions, MR-1 [NiFe]-H_2ase is expressed only under anaerobic conditions (4, 26). In addition, [NiFe]-H_2ase is a heterodimer in which the large subunit contains the catalytic site and the small subunit is a [FeS]-containing protein. The catalytic site has one Ni and one Fe atom. While the Ni atom is coordinated by four cysteine residues, the Fe atom is coordinated by a CO ligand, two CN ligands, and two cysteine residues that are shared with the Ni atom. The small subunit possesses three [FeS] centers that serve as a pathway for transferring electrons between the active site, which is buried deeply inside the enzyme, and the enzyme surface. A group of proteins is directly involved in biosynthesis of the CO and CN ligands and the [FeS] centers, insertion of the Ni, Fe, CO, and CN into the active site of the large subunit, and insertion of [FeS] centers into the small subunit (for reviews, see references 9 and 14). Because of its expression only under anaerobic conditions and the requirement of coexpressing maturation proteins, purification of enough MR-1 [NiFe]-H_2ase, either from MR-1 or from *Escherichia coli* after its heterologous expression, that is enzymatic active for characterization is challenging.

In this report, we cloned the genes encoding MR-1 [NiFe]-H_2ase into a protein expression vector, pBAD202D-TOPO (Invitrogen, Carlsbad, CA), used previously in MR-1 (36, 38).

* Corresponding author. Mailing address: Microbiology Group, Pacific Northwest National Laboratory, 902 Battelle Blvd., MSIN: J4-18, Richland, WA 99352. Phone: (509) 371-6967. Fax: (509) 372-1632. E-mail: liang.shi@pnnl.gov.
▽ Published ahead of print on 1 July 2011.

TABLE 1. MR-1 strains, plasmids, and primers used in this study

Strain, plasmid, or primer	Relevant genotype, description, or sequence (5′ to 3′)	Source, reference, or purpose
Strains		
MR-1	Wild type	ATCC
ΔS02098-ΔSO3920	Δ*hyaB*-Δ*hydA*	24
LS484	Δ*hyaB*-Δ*hydA* plus p*hydA* of *Chlamydomonas reinhardtii*	This study
LS498	Δ*hyaB*-Δ*hydA* plus p*hyaAB*	This study
Plasmids		
pBBR-hydA1N	Coding sequence for *hydA* of *C. reinhardtii*	39
pLS189	Coding sequence for *hyaAB*	This study
Primers		
SO2099ef	CACCTAAGAAGGAGATATACATCCCATGGACACACATGCAGCCC	Construction of pLS189
SO2098er1	TTATTGACCATTGGGGCTG	Construction of pLS189
SO2099RGSer	GTGATGATGGTGATGATGTGAACCCCTCATGGGTTATTCCTCCAGCGG	Construction of pLS189
SO2098RGSef	AGGGGTTCACATCATCACCATCATCACATGAGCAAGCGCGTTGTTATC	Construction of pLS189

Following its introduction into an MR-1 mutant in which the genes encoding the large subunits of [FeFe]-H_2ase and [NiFe]-H_2ases were deleted, the construct restored the mutant's ability to produce H_2 to the level of 37% of that for the MR-1 wild type (wt). MR-1 [NiFe]-H_2ase was purified after expression under the conditions similar to those for heterologous expression of an algal [FeFe]-H_2ase (39), and purified [NiFe]-H_2ase could couple oxidation of H_2 to $Tc(VII)O_4^-$ reduction, demonstrating that purified MR-1 [NiFe]-H_2ase is a functional enzyme that reduces $Tc(VII)O_4^-$ directly.

MATERIALS AND METHODS

Standard procedures. Protein concentrations were measured with a bicinchoninic acid (BCA) protein assay kit from Pierce (Rockford, IL). Sodium dodecyl sulfate-polyacrylamide gel electrophoresis (SDS-PAGE) and Western blot analysis were conducted according to the instructions from Invitrogen (Carlsbad, CA). To visualize proteins directly, gels were stained with GelCode blue stain from Pierce. RGSH epitope-specific antibody is used for detecting the MR-1 hydrogenase tagged with RGSHHHHHH by Western blot analysis (Qiagen, Valencia, CA). Kanamycin is used at 50 μg/ml.

Gene cloning. MR-1 *hyaA* (locus tag SO2099) and *hyaB* (SO2098), the genes encoding respective small and large subunits of [NiFe]-H_2ase, were amplified by PCR with primers S02099ef/SO2099RGSer and SO2098RGSef/SO2098er1, respectively (Table 1). The primers SO2099RGSer and SO2098RGSef contained an overlapping sequence encoding RGSHHHHHH that was fused to the N terminus of the large subunit. The resulting PCR products then served as new templates for the second round of PCR to amplify the entire coding region of *hyaA* and *hyaB* with primers S02099ef/SO2098er1. The PCR products were cloned into a protein expression vector that was previously used in MR-1 cells to create plasmid pLS189 (36–38). Following verification by sequencing, pLS189 was introduced into an MR-1 mutant in which both *hyaB* and *hydA* (locus tag SO3920; the gene encoding the large subunit of [FeFe]-H_2ase) genes were deleted to create MR-1 strain LS498 (24). pBBR-hydA1N was introduced into the same mutant to create LS484 (39). The MR-1 strains, plasmids, and primers used in this study are listed in Table 1.

Measurement of H_2 formation. MR-1 and its various modified strains used were routinely cultured aerobically in LB at 30°C. To measure H_2 formation, all strains were grown in 50 ml of minimal medium with 20 mM lactate as the electron donor and 10 mM formate as the sole electron acceptor in 120-ml serum bottles at 30°C for 72 h (26). The H_2 level in the headspace of serum bottles was measured using a Hewlett-Packard 5890 Series II gas chromatograph (GC) with a thermal conductivity detector (Palo Alto, CA). The GC was fitted with a Supelco 4.572-m by 0.3175-cm stainless-steel support column with Carboxen 1000 60/80 mesh. Ultrapure N_2 was used as the carrier gas. One-milliliter injection aliquots were taken from the serum bottle headspace using a gas-tight glass syringe that was prepurged with N_2. The ultrapure H_2 was used as a standard to determine the amount of H_2 in the headspace of serum bottles. Based on Henry's law, the H_2 concentration in the *Shewanella* liquid cultures was then calculated (18).

Purification of MR-1 [NiFe]-H_2ase. LS498 was grown anaerobically in M72 medium supplemented with 20 mM lactate, 20 mM HEPES, pH 7.8, 1 mM $NiCl_2$, and 10 mM dimethyl sulfoxide (DMSO) at 30°C with agitation (150 rpm) until its optical density at 600 nm reached 0.6 (39). L-Arabinose was added to give a final concentration of 1 mM. The LS498 cells were grown for another 17 h and then harvested by centrifugation at 6,000 × *g* at 4°C for 15 min. The harvested cells were washed once with ice-cold buffer A (20 mM HEPES, pH 7.8, 150 mM NaCl,) and stored at −20°C. Frozen cell pellets were resuspended in buffer B (buffer A plus protease inhibitor [Roche Diagnostic, Indianapolis, IN]) at a ratio of 5 ml/g (wet weight) of cells. The cells were lysed by passage through a French press three times at 8,000 lb/in^2. The unbroken cells and debris were removed by centrifugation at 15,000 × *g* for 30 min. The supernatant was transferred to ultracentrifugation tubes and further centrifuged at 150,000 × *g* for 1 h. Following centrifugation, the supernatant was loaded on to a column of Ni-nitrilotriacetic acid (NTA) agarose preequilibrated with buffer B. The column was washed with buffer B, buffer C (buffer B plus 10 mM imidazole plus 10% [vol/vol] glycerol], and buffer D (buffer C plus 30 mM imidazole), and MR-1 [NiFe]-H_2ase was eluted with buffer E (buffer C plus 240 mM imidazole). The isolated MR-1 [NiFe]-H_2ase was pooled, changed to buffer F (buffer B plus 10% glycerol), and aliquoted in serum bottles in which the headspaces were filled with H_2, and the bottles then stored at −20°C. The purification was conducted at 4°C under aerobic conditions.

Reduction of Tc(VII) by the purified MR-1 [NiFe]-H_2ase. Tc(VII) reductions were performed in 6-ml glass serum vials where 2 ml of reaction solutions containing either HEPES (50 mM, pH 7.8 or 8) or Tris buffer (50 mM, pH 8 at room temperature and 7.8 at 30°C) and 10 μg/ml of purified MR-1 [NiFe]-H_2ase were assembled inside a Coy anaerobic glove bag (95% N_2, 5% H_2, <20 ppm O_2). As a negative control, MR-1 [NiFe]-H_2ase was omitted, while a positive control consisted of methyl viologen added at final concentration of 1 mM. The vials were sealed with butyl rubber stoppers and were then transferred to a fume hood and purged for ~15 min with 0.2-μm filtered, O_2 scrubbed, 100% H_2 (60 lb/in^2) via 22-gauge needles. In another negative control, the H_2 purging step was omitted, and the samples were purged with 100% N_2 instead. Following H_2 or N_2 purging, vials were incubated at 30°C for ~30 min, at which point the reduction of methyl viologen was evident by a visible blue color in the positive-control vials. The rates for reducing methyl viologen by MR-1 [NiFe]-H_2ase in both Tris and HEPES buffers were measured by monitoring the changes of reaction solutions at 605 nm (16). Samples were then transferred to a 30°C Forma anaerobic glove box (95% N_2, 5% H_2, <20 ppm O_2), where 0.2 ml of H_2-purged, anoxic 11 mM $NH_4{}^{99}TcO_4$ in double-distilled H_2O (ddH_2O) was added via a 1-ml syringe and a 22-gauge needle. The vials were placed on a rotisserie shaker (Labquake; Barnstead Thermolyne, Dubuque, IA) in the 30°C glove box. At predetermined time points, 0.3 ml of reaction solution was removed from each vial and added to a 0.5-ml Eppendorf tube. Following vortexing for 15 s, 0.1 ml of reaction solution in the Eppendorf tubes was individually filtered through Nanosep centrifugal filters with molecular mass cutoff of 3 kDa (i.e., 3-kDa filters) by centrifugation at 12,000 × *g* for 7.5 min. After centrifugation, 0.03 ml filtrate was added to 0.57 ml of 4 mM tetraphenyl arsonium chloride (TPAC) in 1.7-ml

Eppendorf tubes to stop the enzymatic reaction and to complex remaining $Tc(VII)O_4^-$. The TPAC-containing solutions were then extracted with chloroform, and the ^{99}Tc in the aqueous phase [i.e., Tc(IV)/Tc(V)] and organic phase [i.e., Tc(VII)] were determined by liquid scintillation counting (LSC) with a Wallac 1414 liquid scintillation counter (Perkin-Elmer, Waltham, MA) (33). The unfiltered samples and the remaining filtrates were subsampled for total ^{99}Tc via LSC in an Optifluor liquid scintillation cocktail. To check residual H_2ase activity after $Tc(VII)O_4^-$ reduction, methyl viologen was added to the remaining solution at final concentration of ~1 mM and change of solution color was monitored at 605 nm for at least 2 h.

TEM. All sample preparation steps were carried out in the Forma anaerobic chamber. About 3 μl of suspension from the Tc samples reduced in HEPES buffer with obvious precipitates was applied to copper grids, dried, and then examined at 120 kV using a Tecnai T12 transmission electron microscope (TEM) equipped with LaB6 filament (FEI, Hillsboro, OR). Images were digitally collected and analyzed using Digital-Micrograph software (Gatan, Inc., Pleasanton, CA). Elemental analysis was performed using an energy-dispersive X-ray spectroscopy (EDX) system (Oxford Instruments, Abingdon, United Kingdom) equipped with a SiLi detector coupled to the JEOL 2010 high-resolution TEM, and spectra were analyzed with ISIS software.

X-ray absorption spectroscopy. For the Tris-buffered sample, a 0.2-μm cellulose nitrate filter paper was soaked in the sample contained in a 1.7-ml Eppendorf tube for 10 min. The remaining liquid was withdrawn and the filter paper placed in a desiccator within the glove bag for 2 days. After drying, the filter paper was cut into sections and placed in an X-ray absorption spectroscopy (XAS) sample holder. For the HEPES-buffered sample, Tc precipitates were collected on the 3-kDa centrifugal filters and then dried for 2 days as described above. Both samples were mixed with boron nitride as a filler and were packed into a 19-mm by 25.4-mm by 2-mm Teflon holder with a 2-mm by 5-mm slot cut through the center, with Kapton adhesive tape (CS Hyde, Co., Lake Villa, IL) applied to one side of the holder to make a recess for the sample. The sample surfaces were checked for smearable radioactive contamination before the samples were sealed inside a Kapton envelope. Inside the Coy glove bag, each sample was placed inside a separate 100-ml glass bottle (Pyrex) sealed with a butyl rubber stopper designed for anaerobic use (Wheaton Science Products, Millville, NJ) and shipped to the Advanced Photon Source at Argonne National Laboratory. The Tc K-edge spectra were obtained at beamline 20-BM at the Advanced Photon Source. At the beamline, the doubly contained samples were kept under flowing He gas to minimize the chance for oxygen exposure by diffusion through the Kapton. The data were obtained in unfocused mode using a 0.8-mm vertical slit. This gave an energy resolution of ~4 eV. An Rh-coated mirror operated at 2.6 millirads provided harmonic rejection. The data were collected in fluorescence mode using a 13-element Ge detector. The energy scale was calibrated using an Mo foil and was occasionally checked to ensure that there were no calibration shifts. All data processing was done using the Athena and Artemis interfaces to the IFFEFFIT software package (34). The data collected were compared to the data from Tc(V)-citrate (provided by Nancy Hess) and $Tc(IV)O_2 \cdot nH_2O$ standards measured previously at the same beamline under similar conditions (43).

RESULTS

Complementation of an MR-1 mutant deficient in H_2 formation. MR-1 possesses two different H_2ases, a [NiFe]-H_2ase and a [FeFe]-H_2ase, which both produce H_2. Deleting the genes encoding both H_2ases abolished MR-1's ability to produce H_2 (26, 39), which provided a clean background for testing whether expressed MR-1 [NiFe]-H_2ase was functional *in vivo*. We transformed an MR-1 mutant in which both *hyaB* and *hydA* genes were deleted (i.e., Δ*hyaB*-Δ*hydA*) with pLS189 that contained the genes encoding MR-1 [NiFe]-H_2ase (i.e., *hyaA* and *hyaB*). The Δ*hyaB*-Δ*hydA* mutant was also transformed with pBBR-hydA1N that contained a gene encoding the [FeFe]-H_2ase of *Chlamydomonas reinhardtii*. Because pBBR-hydA1N was previously shown to produce H_2 in a similar MR-1 mutant, the resulting MR-1 strain served as a positive control for H_2 formation (Table 1) (39).

MR-1 wt, the Δ*hyaB*-Δ*hydA* mutant, and the mutant complemented with pLS189 and pBBR-hydA1N were cultured anaerobically in minimal medium with 20 mM lactate as the electron donor and 10 mM formate as the electron acceptor (26). At 72 h after culturing, 16 ± 3 μM (n = 3) of H_2 was detected in wt culture, while no H_2 was detected in the Δ*hyaB*-Δ*hydA* mutant culture. At the same time, in *trans* complementation of the Δ*hyaB*-Δ*hydA* mutant with MR-1 [NiFe]-H_2ase or [FeFe]-H_2ase of *C. reinhardtii* restored the Δ*hyaB*-Δ*hydA* mutant's ability to produce H_2 at 37% and 45% of that for wt, respectively (Fig. 1). These results provide the first line of evidence that expressed recombinant MR-1 [NiFe]-H_2ase is a functional enzyme that catalyzes H_2 formation *in vivo*.

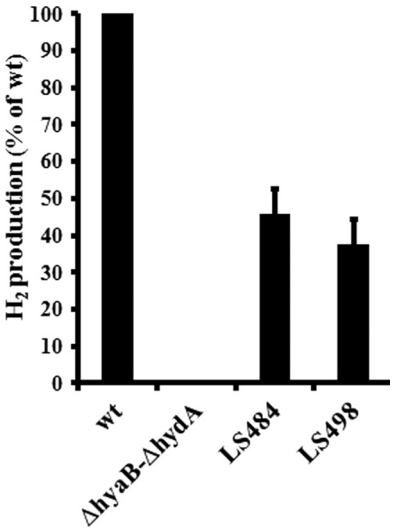

FIG. 1. Complementation of the Δ*hyaB*-Δ*hydA* mutant in H_2 formation. Formations of H_2 by the wt, the Δ*hyaB*-Δ*hydA* mutant, and the LS484 (Δ*hyaB*-Δ*hydA* plus p*hydA* of *C. reinhardtii*) and LS498 (Δ*hyaB*-Δ*hydA* plus p*hyaAB*) mutants was measured as described in Materials and Methods. The 100% H_2 formation by the wt was 16 ± 3 μM (n = 3).

Purification of MR-1 [NiFe]-H_2ase. To purify MR-1 [NiFe]-H_2ase, it was expressed in the Δ*hyaB*-Δ*hydA* mutant when 10 mM DMSO was used as the terminal electron acceptor (39). Following cell lysis and ultracentrifugation, the MR-1 [NiFe]-H_2ase was isolated from the supernatant by using immobilized metal ion affinity chromatography. The purified MR-1 [NiFe]-H_2ase migrated as two bands with nearly equimolar stoichiometries on SDS-PAGE, with apparent masses of 41 and 62 kDa, respectively (Fig. 2). The apparent mass of 62 kDa is consistent with the calculated molecular mass of the large subunit, while the mass of 41 kDa is more than the calculated mass for the matured small subunit, which is ~33 kDa. However, it is not surprising that the apparent molecular mass detected by SDS-PAGE is different from that calculated. Deviations from the calculated values of 5 to 20% are common, and "discrepancies" of 2-fold or more were reported for a number of proteins (8). Western blot analysis with anti-RGSH antibody confirmed that the protein with an apparent mass of 62 kDa was the large subunit of MR-1 [NiFe]-H_2ase (data not shown). Thus, purified recombinant MR-1 [NiFe]-H_2ase proteins are nearly electrophoretically homogenous.

$Tc(VII)O_4^-$ reduction by the purified MR-1 [NiFe]-H_2ase. The purified MR-1 [NiFe]-H_2ase was tested for its ability to

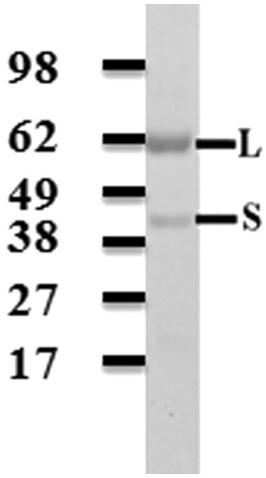

FIG. 2. Purified MR-1 [NiFe]-H_2ase. SDS-PAGE (8 to 12% [wt/vol] acrylamide gradient) demonstrating electrophoretic purity of purified MR-1 [NiFe]-H_2ase (~1 μg). Migration positions of protein standards are indicated at the left.

couple H_2 oxidation to $Tc(VII)O_4^-$ reduction. When 50 mM Tris (pH 8 at room temperature and 7.8 at 30°C) was used as the buffer, purified MR-1 [NiFe]-H_2ase completed $Tc(VII)O_4^-$ reduction within 24 h. No $Tc(VII)O_4^-$ reduction occurred when MR-1 [NiFe]-H_2ase or H_2 was omitted. At 24 h, while the control solution in which H_2 was omitted was colorless (Fig. 3A), the reaction solution in the presence of H_2 became pink, with an absorption peak at 512 nm. In addition, no apparent precipitate was observed in this reaction solution, and the solution was easily passed through the 3-kDa filters (Fig. 3B). In contrast to that in Tris buffer, $Tc(VII)O_4^-$ reduction by MR-1 [NiFe]-H_2ase in 50 mM HEPES (pH 8) was incomplete after 2 days. At 24 h, only 20% of $Tc(VII)O_4^-$ was reduced, the reaction solution became brown, and black precipitates were visible (Fig. 3C). Modest change of the pH of HEPES buffer from 8 to 7.8 did not alter the incomplete

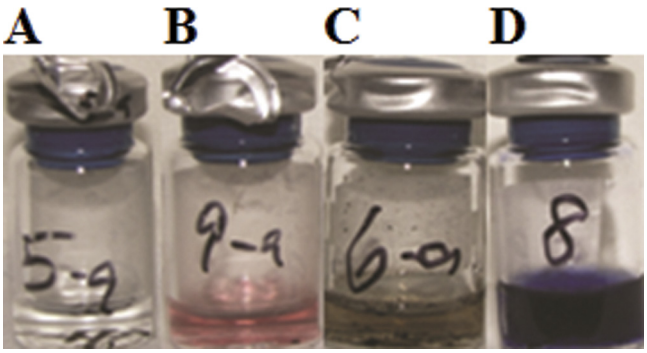

FIG. 3. Reduction of $Tc(VII)O_4^-$ and methyl viologen by the purified MR-1 [NiFe]-H_2ase. Reduction assays were carried out as described in Materials and Methods. (A) Negative control: $Tc(VII)O_4^-$ mixed with MR-1 [NiFe]-H_2ase in Tris buffer without H_2. (B) $Tc(VII)O_4^-$ reduction by MR-1 [NiFe]-H_2ase in Tris buffer with H_2. (C) $Tc(VII)O_4^-$ reduction by MR-1 [NiFe]-H_2ase in HEPES buffer with H_2. (D) Positive control: methyl viologen reduction by MR-1 [NiFe]-H_2ase in HEPES buffer with H_2. Formation of reduced methyl viologen (blue) is evident.

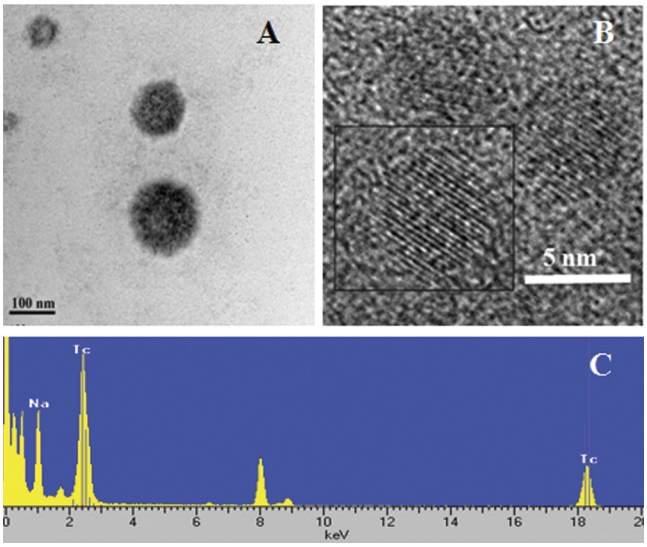

FIG. 4. TEM examination of reduced Tc by MR-1 [NiFe]-H_2ase in HEPES buffer. (A) Formation of round electron-dense particles was evident. (B) These particles were packed with crystallites. (Inset) Examination of a crystallite at high resolution. (C) EDX spectrum indicating the presence of Tc in the electron-dense particles found in panel A.

reduction of Tc(VII) (data not shown), and in all cases, the black precipitates were retained by the 3-kDa filters. In addition to $Tc(VII)O_4^-$, MR-1 [NiFe]-H_2ase could also couple H_2 oxidation to reduction of methyl viologen, an artificial electron acceptor, in both Tris and HEPES buffers (Fig. 3D). Buffer type did not affect MR-1 [NiFe]-H_2ase-mediated methyl viologen reduction significantly, because the reduction rates were 17.0 ± 0.1 nmol min^{-1} mg^{-1} ($n = 3$) in Tris buffer (pH 7.8) and 17.4 ± 0.2 nmol min^{-1} mg^{-1} ($n = 3$) in HEPES buffer (pH 7.8). The residual H_2ase activity after $Tc(VII)O_4^-$ reduction was, thus, determined by addition of methyl viologen in the reaction solutions at 2 days after reduction of $Tc(VII)O_4^-$. In Tris buffer, change of absorbance of reaction solution at 605 nm could be detected at 10 min after addition of methyl viologen, and residual activity for reducing methyl viologen was 0.79 ± 0.01 nmol min^{-1} mg^{-1} ($n = 3$). In HEPES buffer, however, no change of absorbance of reaction solution at 605 nm could be detected at 2 h. All these results demonstrate that purified MR-1 [NiFe]-H_2ase is a functional enzyme that couples H_2 oxidation to reduction of $Tc(VII)O_4^-$ and methyl viologen and reduction of $Tc(VII)O_4^-$ in HEPES buffer rapidly inactivates the reduction activity of MR-1 [NiFe]-H_2ase.

TEM characterization of reduced Tc. To further characterize MR-1 [NiFe]-H_2ase-mediated $Tc(VII)O_4^-$ reduction, the reduced Tc products in HEPES buffers were examined by TEM. Round electron-dense particles ranging from 30 to 80 nm in diameter were imaged by TEM (Fig. 4A). Examination of the particles at high resolution revealed that they were aggregates of individual crystallites with diameters of ~5 nm (Fig. 4B). EDX analyses of these electron-dense particles confirmed that they were rich in Tc (Fig. 4C).

XAS characterization of reduced Tc. The Tc products reduced in both Tris and HEPES buffers were also analyzed by XAS. As shown in Fig. 5, X-ray absorption near-edge spectros-

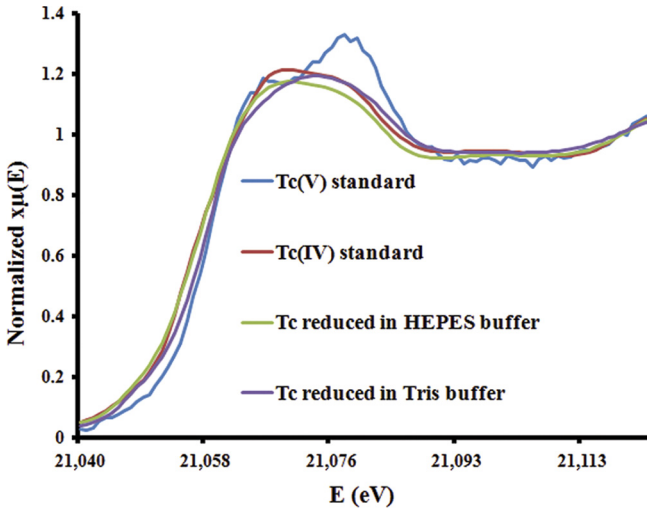

FIG. 5. XANES spectra of the standards of Tc(V) citrate and $Tc(IV)O_2 \cdot nH_2O$ and Tc reduced by MR-1 [NiFe]-H_2ase in Tris and HEPES buffers.

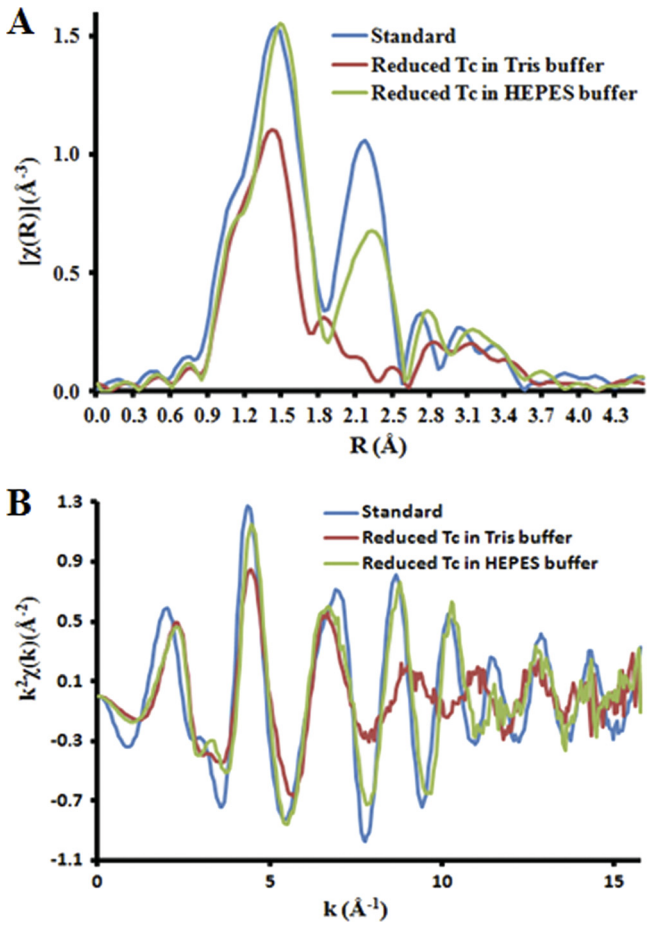

FIG. 6. EXAFS (A) and transform of the EXAFS (B) spectra of the $Tc(IV)O_2 \cdot nH_2O$ standard and Tc reduced by MR-1 [NiFe]-H_2ase in Tris and HEPES buffers.

copy (XANES) measurements revealed that, compared to the standards of Tc(IV) and Tc(V), the Tc product reduced in HEPES buffer was Tc(IV). For those in Tris buffer, there was clearly a shift of the edge indicating the presence of more-oxidized forms of Tc. The Tc(V) standard was not a good match to the shape of the first peak, but fitting the near edge with linear combinations of Tc(IV), Tc(V), and Tc(VII) typically gave 30 to 50% Tc(V) and 0.1% Tc(VII) with the balance of Tc(IV). Both extended X-ray adsorption fine structure (EXAFS) (Fig. 6A) and the Fourier transform of the EXAFS (Fig. 6B) measurements also revealed the structural difference between the products reduced in these two buffers. For the $Tc(IV)O_2 \cdot nH_2O$ standard used, the first peak in the Fourier transform EXAFS spectrum arose from Tc-O near neighbor bonds, and the second peak was indicative of Tc-Tc bonds (Fig. 6B) (22). The $TcO_2 \cdot nH_2O$ standard consists of extended chains of edge-sharing Tc-O octahedral, giving rise to the Tc-O first peak and the short Tc-Tc second-neighbor bonds. The Fourier transform of the EXAFS spectrum of Tc(IV) reduced in HEPES buffer was very similar to that of standard $Tc(IV)O_2 \cdot nH_2O$, with the main difference being a reduction in the Tc-Tc peak. Shorter chains of Tc-O octahedral resulting in a reduced number of Tc-Tc bonds might contribute to the reduction of the Tc-Tc peak. Nevertheless, the basic Tc-O octahedral unit of the Tc(IV) in HEPES buffer is nearly the same of that of standard $Tc(IV)O_2 \cdot nH_2O$. The Fourier transform EXAFS spectrum of the Tc reduced in Tris buffer was distinctly different from that for the Tc(IV) reduced in HEPES buffer. It showed that the Tc-Tc signal was absent and the Tc-O peak was reduced. The first shell peak was well described by 3 or 4 O neighbors at 1.97 Å (Fig. 6B). This indicates that the Tc environments in the two samples are very different.

DISCUSSION

Critical to the identification of the possible role of MR-1 [NiFe]-H_2ase in catalyzing Tc(VII) reduction is the ability to express functional hydrogenase enzyme, which was possible by expressing MR-1 [NiFe]-H_2ase under the conditions similar to those for the heterologous expression of [FeFe]-H_2ase (39). Our results demonstrate that MR-1 is an efficient host for homologous expression of recombinant MR-1 [NiFe]-H_2ase, which greatly facilitates purification and subsequent mechanistic characterization. In previous studies, MR-1 [NiFe]-H_2ase was implicated in H_2 oxidation and formation and in H_2-driven Tc(VII) reduction *in vivo* (24, 26). In this study, we demonstrate that expression of MR-1 [NiFe]-H_2ase complements a hydrogenase-deficient mutant's ability to form H_2 and that purified MR-1 [NiFe]-H_2ase can directly oxidize H_2 and use the released electrons to reduce Tc(VII) to Tc(IV).

In previous study, when $Tc(VII)O_4^-$ was reduced in 50 mM Tris buffer (pH 8) by purified [NiFe]-H_2ase of *Desulfovibrio fructosovorans*, no visible precipitate was observed, the reaction solution was pink, and the reduction product was Tc(V). However, when it was reduced in 20 mM morpholinepropanesulfonic acid (MOPS) buffer (pH 6.5), brown precipitates were visible, but the chemical nature of the precipitates was never analyzed (12). In this study, when $Tc(VII)O_4^-$ was reduced in 50 mM Tris buffer (pH 7.8) by purified MR-1[NiFe]-H_2ase, no visible precipitate was observed, the reaction solution was pink, and reduction products were a mixture of Tc(IV) and Tc(V).

When it was reduced in 50 mM HEPES buffer (pH 7.8), black precipitates were visible and the reduction product was $Tc(IV)O_2 \cdot nH_2O$. The difference between this and previous studies in terms of oxidation states of reduced Tc products in Tris buffer may be attributed to the different enzymes used for $Tc(VII)O_4^-$ reductions and the different methods used for analyzing the reduced products. Unlike for a previous study in which different buffers with different concentrations and different pHs were used, we used Tris and HEPES buffers with the same concentration and pH for the $Tc(VII)O_4^-$ reduction assay in this study. Thus, it is the different type of buffers that contributes to the different reduction rates and products observed in this study.

$Tc(IV)O_2 \cdot nH_2O$ precipitates are the products of $Tc(VII)O_4^-$ reduction by MR-1 cells (24). TEM analysis shows that Tc(IV) precipitates reduced in HEPES buffer are the aggregates packed with ~5-nm-diameter crystallites. XAS analysis confirmed that the crystallites consist of $Tc(IV)O_2 \cdot nH_2O$. To the best of our knowledge, this is the first report of enzyme-mediated formation of $Tc(IV)O_2 \cdot nH_2O$ crystallites whose aggregations result in formation of Tc(IV) precipitates. The exact bonding environment of the Tc(V)/Tc(IV) reduced in Tris buffer could not be determined in this study, because of the lack of a structural model and appropriate standards for Tc(V)/Tc(IV)-Tris bonding. However, Tc(IV) complexed by bicarbonate, EDTA, or glyoxylic acid is soluble and pink, with absorbance peaks at 500 to 512 nm (22, 32). Compared to HEPES, Tris is a better complexing ligand for Cr(III) (5). In addition to Cr(III), Tris also complexes Co(III) (1). Given that the Tc(V)/Tc(IV) reduced in Tris buffer are soluble and pink, with absorbance peak at 512 nm, exhibit changes in the Tc-O bonding compared to $Tc(IV)O_2 \cdot nH_2O$ standard, and contain no Tc-Tc bond, it is reasonable to speculate that Tris may have complexed Tc(V)/Tc(IV) and prevented them from forming crystallites.

It should be noted that, unlike those observed *in vitro*, buffer types have no impact on *in vivo* reduction of $Tc(VII)O_4^-$ by *D. fructosovorans* and that Tc precipitates were detected in the cells buffered with Tris (12). This suggests that the periplasm of *D. fructosovorans*, where [NiFe]-H_2ase is located, may lack enough ligands for complexing the Tc(V) produced. In MR-1 cells, $Tc(IV)O_2 \cdot nH_2O$ precipitates were found on the bacterial cell surface and in the periplasm. Deletion of the *hyaB* gene eliminates $Tc(IV)O_2 \cdot nH_2O$ precipitates found in the periplasm but not on the cell surfaces, where $Tc(VII)O_4^-$ reduction is mediated by MR-1 outer membrane cytochromes MtrC and OmcA (24). Given that MR-1 [NiFe]-H_2ase is required for *in vivo* reduction of $Tc(VII)O_4^-$, that purified [NiFe]-H_2ase directly reduces $Tc(VII)O_4^-$ *in vitro*, and that $Tc(IV)O_2 \cdot nH_2O$ precipitates are the same product of both *in vivo* and *in vitro* reductions, it is reasonable to conclude that (i) MR-1 [NiFe]-H_2ase can serve as the terminal reductase for *in vivo* reduction of $Tc(VII)O_4^-$, (ii) the MR-1 periplasm may also lack endogenous ligands for complexing the reduced Tc products, and (iii) HEPES is a relevant buffer for investigating *in vitro* $Tc(VII)O_4^-$ reduction.

MR-1 [NiFe]-H_2ase is located in the periplasm, where $Tc(VII)O_4^-$ is probably transported in via MR-1 transport proteins similar to those found in plant roots (7). During H_2 oxidation-coupled reduction of $Tc(VII)O_4^-$, H_2 molecules diffuse into the active center that is buried deeply inside the protein via a H_2 channel. Following H_2 oxidation, the protons and electrons are transported to the enzyme surface via a proton channel and an electron transfer chain, respectively (11). The released H^+ is most likely transported into the cytoplasm by H^+ transporters, such as ATP synthase, located in the cytoplasmic or inner membrane. Because the electron transfer chain is located within the small subunit, we hypothesize that $Tc(VII)O_4^-$ reduction occurs at the exit point of the electron transfer chain on the surface of the small subunit (Fig. 7). The reduced Tc(IV) forms $Tc(IV)O_2 \cdot nH_2O$ precipitates probably due to lacking complexing ligands in the periplasm. Likewise, the low complexing capability of HEPES may contribute in part to Tc(IV) precipitation *in vitro*. MR-1 [NiFe]-H_2ase may be adsorbed to the surface of $Tc(IV)O_2 \cdot nH_2O$ precipitates, and adsorption of MR-1 [NiFe]-H_2ase to $Tc(IV)O_2 \cdot nH_2O$ precipitates may block the access of H_2 to the H_2 channel and/or transfer of protons and electrons to the surrounding solution and Tc(VII), respectively, rendering hydrogenase less reactive. In Tris buffer, the reduced Tc(V)/Tc(IV) remains soluble, probably through complexation by Tris, which results in a quick reduction of Tc(VII) by the hydrogenase. Future research will focus on testing these hypotheses. Because they are found in the MR-1 periplasm, $Tc(IV)O_2 \cdot nH_2O$ precipitates may also have inhibitory effects on [NiFe]-H_2ase activity *in vivo*.

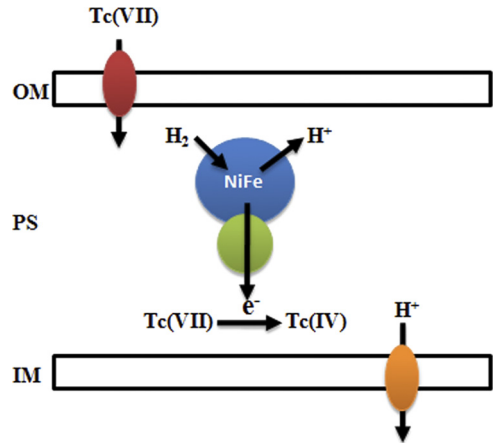

FIG. 7. Model of MR-1 [NiFe]-H_2ase-mediated $Tc(VII)O_4^-$ reduction. Through transporter proteins (red circle) in the bacterial outer membrane (OM), $Tc(VII)O_4^-$ is transported into the periplasm (PS), where [NiFe]-H_2ase is located. During H_2 oxidation-coupled reduction of $Tc(VII)O_4^-$, H_2 molecules diffuse into the NiFe active center that is buried deeply inside the hydrogenase (blue circle, large subunit; green circle, small subunit) via a H_2 channel. After oxidation, the released protons are transported out of the hydrogenase through a proposed proton channel into the PS, where they can be transported into the cytoplasm through H^+ transporters (orange circle) located in the cytoplasmic or inner membrane (IM). The released electrons are transferred via a chain of [FeS] centers located within the small subunit to the surface of the small subunit, where $Tc(VII)O_4^-$ reduction occurs. Arrows indicate the directions of $Tc(VII)O_4^-$, H_2, proton (H^+), and electron (e^-) movements and reduction of $Tc(VII)O_4^-$ to Tc(IV).

In summary, by using MR-1 as a host, MR-1 [NiFe]-H_2ase is homologously expressed under the conditions similar to those for expressing an algal [FeFe]-H_2ase and then purified. The purified protein is a terminal reductase that couples H_2 oxida-

tion to Tc(VII) reduction. MR-1 [NiFe]-H_2ase-mediated Tc(VII) reduction is influenced by the buffers used. Under the conditions tested, Tc(VII) reduction is complete, no visible Tc precipitate is formed, and reduction products are a mixture of Tc(IV) and Tc(V) in Tris buffer, while in HEPES buffer, reaction is incomplete, and reduction products are $Tc(IV)O_2 \cdot nH_2O$ crystallites that form aggregates. These different outcomes of MR-1 [NiFe]-H_2ase-mediated Tc(VII) reduction may be attributed to different complexing capabilities for the reduced Tc products between Tris and HEPES. Because $Tc(IV)O_2 \cdot nH_2O$ precipitates are also detected in the MR-1 periplasm, HEPES should be used for *in vitro* investigation of MR-1 [NiFe]-H_2ase-mediated Tc(VII) reduction.

ACKNOWLEDGMENTS

This research was supported by the Subsurface Biogeochemical Research program (SBR)/Office of Biological and Environmental Research (BER) and Physical Bioscience program/Office of Basic Energy Science (BES), U.S. Department of Energy (DOE). A portion of the research was performed using EMSL, a national scientific user facility sponsored by the DOE-BER and located at Pacific Northwest National Laboratory (PNNL). PNNL is operated for the DOE by Battelle under contract DE-AC05-76RLO 1830. Use of the Advanced Photon Source is supported by the DOE-BES under contract DE-AC02-06CH11357.

REFERENCES

1. **Allen, D. E., D. J. Baker, and R. D. Gillard.** 1967. Metal complexing by Tris buffer. Nature **214:**906–907.
2. **Belchik, S. M., et al.** 2011. Extracellular reduction of hexavalant chromium by cytochromes MtrC and OmcA of *Shewanella oneidensis* MR-1. Appl. Environ. Microbiol. **77:**4035–4041.
3. **Beliaev, A. S., D. A. Saffarini, J. L. McLaughlin, and D. Hunnicutt.** 2001. MtrC, an outer membrane decahaem *c* cytochrome required for metal reduction in *Shewanella putrefaciens* MR-1. Mol. Microbiol. **39:**722–730.
4. **Beliaev, A. S., et al.** 2002. Gene and protein expression profiles of *Shewanella oneidensis* during anaerobic growth with different electron acceptors. OMICS **6:**39–60.
5. **Bencheikh-Latmani, R., A. Obraztsova, M. R. Mackey, M. H. Ellisman, and B. M. Tebo.** 2007. Toxicity of Cr(lll) to *Shewanella* sp. strain MR-4 during Cr(VI) reduction. Environ. Sci. Technol. **41:**214–220.
6. **Bencheikh-Latmani, R., et al.** 2005. Global transcriptional profiling of *Shewanella oneidensis* MR-1 during Cr(VI) and U(VI) reduction. Appl. Environ. Microbiol. **71:**7453–7460.
7. **Bennett, R., and N. Willey.** 2003. Soil availability, plant uptake and soil to plant transfer of ^{99}Tc—a review. J. Environ. Radioact. **65:**215–231.
8. **Bischoff, K. M., L. Shi, and P. J. Kennelly.** 1998. The detection of enzyme activity following sodium dodecyl sulfate-polyacrylamide gel electrophoresis. Anal. Biochem. **260:**1–17.
9. **Casalot, L., and M. Rousset.** 2001. Maturation of the [NiFe] hydrogenases. Trends Microbiol. **9:**228–937.
10. **Clarke, T. A., et al.** 2008. The role of multihaem cytochromes in the respiration of nitrite in *Escherichia coli* and Fe(III) in *Shewanella oneidensis*. Biochem. Soc. Trans. **36:**1005–1010.
11. **De Lacey, A. L., V. M. Fernandez, M. Rousset, and R. Cammack.** 2007. Activation and inactivation of hydrogenase function and the catalytic cycle: spectroelectrochemical studies. Chem. Rev. **107:**4304–4330.
12. **De Luca, G., P. de Philip, Z. Dermoun, M. Rousset, and A. Vermeglio.** 2001. Reduction of technetium(VII) by *Desulfovibrio fructosovorans* is mediated by the nickel-iron hydrogenase. Appl. Environ. Microbiol. **67:**4583–4587.
13. **Eggleston, C. M., et al.** 2008. Binding and direct electrochemistry of OmcA, an outer-membrane cytochrome from an iron reducing bacterium, with oxide electrode: a candidate biofuel system. Inorg. Chim. Acta **361:**769–777.
14. **Forzi, L., and R. G. Sawers.** 2007. Maturation of [NiFe]-hydrogenases in *Escherichia coli*. Biometals **20:**565–578.
15. **Fredrickson, J. K., et al.** 2002. Influence of Mn oxides on the reduction of uranium(VI) by the metal-reducing bacterium *Shewanella putrefaciens*. Geochim. Cosmochim. Acta **66:**3247–3262.
16. **Hare, P. M., E. A. Price, and D. M. Bartels.** 2008. Hydrated electron extinction coefficient revisited. J. Phys. Chem. A **112:**6800–6802.
17. **Hartshorne, R. S., et al.** 2007. Characterization of *Shewanella oneidensis* MtrC: a cell-surface decaheme cytochrome involved in respiratory electron transport to extracellular electron acceptors. J. Biol. Inorg. Chem. **12:**1083–1094.
18. **Helmann, A., S. Marczlnek, K. Kloos, and S. Pelffer.** 2003. Optimization of sampling technique for the determination of dissolved hydrogen in groundwater. Acta Hydrochim. Hydrobiol. **31:**491–500.
19. **Johs, A., L. Shi, T. Droubay, J. F. Ankner, and L. Liang.** 2010. Characterization of the decaheme *c*-type cytochrome OmcA in solution and on hematite surfaces by small angle x-ray scattering and neutron reflectometry. Biophys. J. **98:**3035–3043.
20. **Liu, C., Y. A. Gorby, J. M. Zachara, J. K. Fredrickson, and C. F. Brown.** 2002. Reduction kinetics of Fe(III), Co(III), U(VI), Cr(VI), and Tc(VII) in cultures of dissimilatory metal-reducing bacteria. Biotechnol. Bioeng. **80:**637–649.
21. **Liu, C., J. M. Zachara, J. K. Fredrickson, D. W. Kennedy, and A. Dohnalkova.** 2002. Modeling the inhibition of the bacterial reduction of U(VI) by beta-MnO_2(s). Environ. Sci. Technol. **36:**1452–1459.
22. **Lukens, W. W., Jr., J. I. Bucher, N. M. Edelstein, and D. K. Shuh.** 2002. Products of pertechnetate radiolysis in highly alkaline solution: structure of $TcO_2 \cdot$ xH2O. Environ. Sci. Technol. **36:**1124–1129.
23. **Marshall, M. J., et al.** 2006. c-Type cytochrome-dependent formation of U(IV) nanoparticles by *Shewanella oneidensis*. PLoS Biol. **4:**e268.
24. **Marshall, M. J., et al.** 2008. Hydrogenase- and outer membrane *c*-type cytochrome-facilitated reduction of technetium(VII) by *Shewanella oneidensis* MR-1. Environ. Microbiol. **10:**125–136.
25. **Meitl, L. A., et al.** 2009. Electrochemical interaction of *Shewanella oneidensis* MR-1 and its outer membrane cytochromes OmcA and MtrC with hematite electrodes. Geochim. Cosmochim. Acta **2009:**5292–5307.
26. **Meshulam-Simon, G., S. Behrens, A. D. Choo, and A. M. Spormann.** 2007. Hydrogen metabolism in *Shewanella oneidensis* MR-1. Appl. Environ. Microbiol. **73:**1153–1165.
27. **Middleton, S. S., et al.** 2003. Cometabolism of Cr(VI) by *Shewanella oneidensis* MR-1 produces cell-associated reduced chromium and inhibits growth. Biotechnol. Bioeng. **83:**627–637.
28. **Myers, C. R., B. P. Carstens, W. E. Antholine, and J. M. Myers.** 2000. Chromium(VI) reductase activity is associated with the cytoplasmic membrane of anaerobically grown *Shewanella putrefaciens* MR-1. J. Appl. Microbiol. **88:**98–106.
29. **Myers, C. R., and K. H. Nealson.** 1988. Bacterial manganese reduction and growth with manganese oxide as the sole electron acceptor. Science **240:** 1319–1321.
30. **Myers, C. R., and K. H. Nealson.** 1990. Respiration-linked proton translocation coupled to anaerobic reduction of manganese(IV) and iron(III) in *Shewanella putrefaciens* MR-1. J. Bacteriol. **172:**6232–6238.
31. **Myers, J. M., and C. R. Myers.** 2001. Role for outer membrane cytochromes OmcA and OmcB of *Shewanella putrefaciens* MR-1 in reduction of manganese dioxide. Appl. Environ. Microbiol. **67:**260–269.
32. **Paquette, J., and W. E. Lawrence.** 1985. A spectroelectrochemical study of the technetium (IV)/technetium (III) couple in bicarbonate solutions. Can. J. Chem. **63:**2369–2373.
33. **Plymale, A. E., et al.** 2011. Competitive reduction of pertechnetate (^{99}TcO4-) by dissimilatory metal reducing bacteria and biogenic Fe(II). Environ. Sci. Technol. **45:**951–957.
34. **Ravel, B., and M. Newville.** 2005. ATHENA, ARTEMIS, HEPHAESTUS; data analysis for X-ray absorption spectroscopy using IFEFFIT. J. Synchrotron Radiat. **12:**537–541.
35. **Ross, D. E., S. L. Brantley, and M. Tien.** 2009. Kinetic characterization of OmcA and MtrC, terminal reductases involved in respiratory electron transfer for dissimilatory iron reduction in *Shewanella oneidensis* MR-1. Appl. Environ. Microbiol. **75:**5218–5226.
36. **Shi, L., et al.** 2006. Isolation of a high-affinity functional protein complex between OmcA and MtrC: two outer membrane decaheme *c*-type cytochromes of *Shewanella oneidensis* MR-1. J. Bacteriol. **188:**4705–4714.
37. **Shi, L., et al.** 2008. Direct involvement of type II secretion system in extracellular translocation of *Shewanella oneidensis* outer membrane cytochromes MtrC and OmcA. J. Bacteriol. **190:**5512–5516.
38. **Shi, L., J. T. Lin, L. M. Markillie, T. C. Squier, and B. S. Hooker.** 2005. Overexpression of multi-heme C-type cytochromes. Biotechniques **38:**297–299.
39. **Sybirna, K., et al.** 2008. *Shewanella oneidensis*: a new and efficient system for expression and maturation of heterologous [Fe-Fe] hydrogenase from *Chlamydomonas reinhardtii*. BMC Biotechnol. **8:**73.
40. **Wang, Z., et al.** 2008. Kinetics of reduction of Fe(III) complexes by outer membrane cytochromes MtrC and OmcA of *Shewanella oneidensis* MR-1. Appl. Environ. Microbiol. **74:**6746–6755.
41. **Wildung, R. E., et al.** 2000. Effect of electron donor and solution chemistry on products of dissimilatory reduction of technetium by *Shewanella putrefaciens*. Appl. Environ. Microbiol. **66:**2451–2460.
42. **Xiong, Y., et al.** 2006. High-affinity binding and direct electron transfer to solid metals by the *Shewanella oneidensis* MR-1 outer membrane *c*-type cytochrome OmcA. J. Am. Chem. Soc. **128:**13978–13979.
43. **Zachara, J. M., et al.** 2007. Reduction of pertechnetate [Tc(VII)] by aqueous Fe(II) and the nature of solid phase redox products. Geochim. Cosmochim. Acta **71:**2137–2157.